Research

Cell Calcium (1997) **21**(6), 441–452

A high-resolution, confocal laser-scanning microscope and flash photolysis system for physiological studies

Ian Parker[1], Nick Callamaras[1], W. Gil Wier[2]

[1]Laboratory of Cellular and Molecular Neurobiology, Department of Psychobiology, University of California Irvine, California, USA

[2]Department of Physiology, University of Maryland School of Medicine, Baltimore, Maryland, USA

Summary We describe the construction of a high-resolution confocal laser-scanning microscope, and illustrate its use for studying elementary Ca^{2+} signalling events in cells. An avalanche photodiode module and simple optical path provide a high efficiency system for detection of fluorescence signals, allowing use of a small confocal aperture giving near diffraction-limited spatial resolution (< 300 nm lateral and < 400 nm axial). When operated in line-scan mode, the maximum temporal resolution is 1 ms, and the associated computer software allows complete flexibility to record line-scans continuously for long (minutes) periods or to obtain any desired pixel resolution in x–y scans. An independent UV irradiation system permits simultaneous photolysis of caged compounds over either a uniform, wide field (arc lamp source) or at a tightly focussed spot (frequency-tripled Nd:YAG laser). The microscope thus provides a versatile tool for optical studies of dynamic cellular processes, as well as excellent resolution for morphological studies. The confocal scanner can be added to virtually any inverted microscope for a component cost that is only a small fraction of that of comparable commercial instruments, yet offers better performance and greater versatility.

INTRODUCTION

The introduction of confocal laser-scanning microscopes (CLSM), in conjunction with the availability of highly sensitive fluorescent Ca^{2+} indicator dyes, has greatly enhanced our understanding of complex spatio-temporal aspects of intracellular signalling. In particular, the optical-sectioning ability of the confocal microscope [1] has recently allowed the resolution of localized Ca^{2+} transients such as 'puffs' [2,3] and 'sparks' [4], which may represent elementary units of intracellular Ca^{2+} liberation [5]. Because most currently available confocal microscopes were designed primarily for morphological studies of fixed or slowly changing specimens, their use, however, presents several difficulties for investigators wishing to image rapid dynamic cellular signals such as fluorescence Ca^{2+} transients.

First, the optical paths within commercial instruments tend to be complex, and the detectors and associated electronics are often relatively inefficient [6]. These factors lead to a low overall efficiency in detection of emitted photons, and consequently require use of a high laser intensity and/or larger than optimal confocal aperture to obtain images with adequate signal-to-noise ratio. Also, the complexity of the light path makes adjustment difficult for the user, so that CLSM systems are frequently operated with less than optimal alignment. Secondly, the associated control and image processing software may not be written with dynamic studies in mind, so that the user may be unnecessarily constrained in the types of recording possible. For example, the

Received 27 January 1997
Revised 8 April 1997
Accepted 8 April 1997

Correspondence to: Dr Ian Parker, Laboratory of Cellular and Molecular Neurobiology, Department of Psychobiology, University of California Irvine, CA 92697-4550, USA. Tel: +1 714 824 7332; Fax: +1 714 824 2447
E-mail: iparker@uci.edu

available pixel resolutions may be limited and it may be possible to record continuous line-scan data for only short periods. Finally, the high cost of commercial CLSM (usually > US$100 000) makes them difficult to justify by individual investigators.

We describe here the construction and performance of a 'homebrew' confocal laser-scanning system which overcomes the above objections. This system was designed primarily for rapid (up to 1 kHz) linescan imaging of Ca^{2+} puffs and sparks, but also works well for many other applications, including high-resolution two- and three-dimensional imaging. Specific features include use of a simple optical path, an avalanche photodiode detector with high quantum efficiency [7], and true photon-counting circuitry [8]. In conjunction, these provide a high efficiency of detection of emitted fluorescence, so that clear signals are obtained even with small confocal apertures that allow close to diffraction-limited spatial resolution. For example, this instrument has provided linescan images of elementary Ca^{2+} signals (puffs and sparks) with a resolution appreciably better than the BioRad MRC 600 and Noran Odyssey systems operated under similar conditions in the authors' laboratories. Further, the associated software allows the user complete flexibility, with the linescan and x–y image size limited only by computer disc space. The total component cost to add confocal scanning capability to an existing inverted microscope is about US$20 000 (10–20% that of a comparable commercial instrument), and the effort involved is less than might be expected. For example, construction of a duplicate instrument based on the original prototype took only about 3 weeks from unpacking boxes to obtaining images. In addition, we describe the construction and use of a separate UV laser photolysis system, which is employed together with the CLSM to image Ca^{2+} signals evoked by photorelease of intracellular messengers from caged precursors.

MATERIALS AND METHODS

The optical systems described here comprise two independent units; a laser scanner and confocal detector comprising the CLSM and a UV photolysis system. These are constructed using standard 1 inch optical components (New Focus Inc., Sunnyvale, CA, USA) mounted on a 4 × 2.5 ft optical breadboard (Melles Griot, Irvine, CA, USA) and interfaced to an Olympus IX70 inverted microscope through, respectively, the video and epifluorescence ports of the microscope (Fig. 1A). The following sections describe specific details of construction and use. Copies of circuit diagrams and software routines are available from the authors upon request. For more general information pertaining to the principles and applications of biological confocal microscopy see [1].

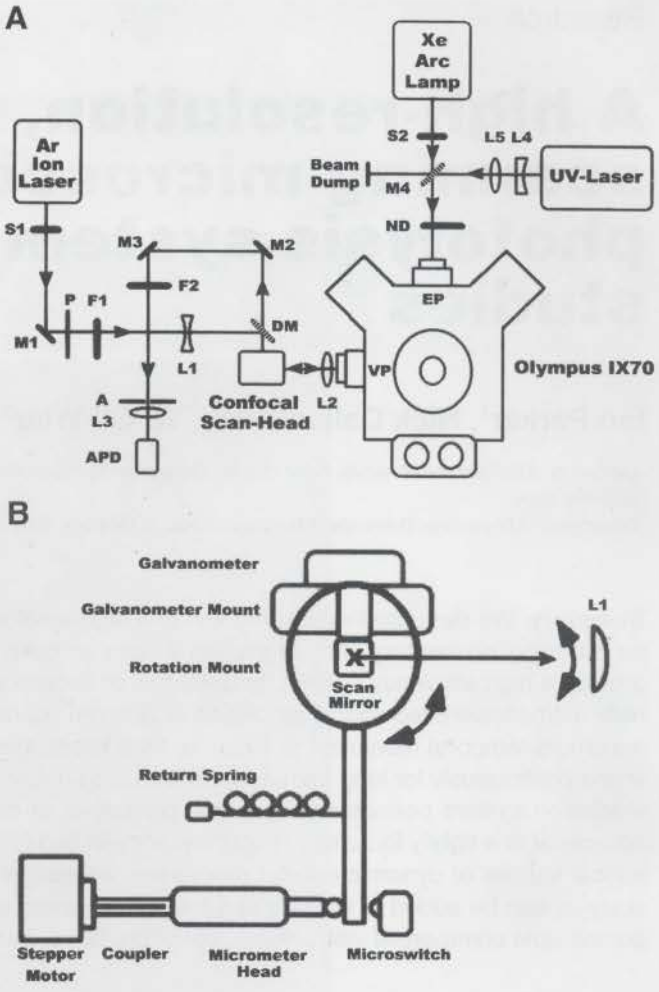

Fig. 1 (**A**) Optical layout of the CLSM and UV photolysis systems. The CLSM is interfaced through the video port (VP) on the left of the Olympus IX70 microscope, and the photolysis system through the epifluorescence port (EP) at the rear of the microscope. S1,2 = shutters; M1–3 = fully reflecting front surface mirrors; P = rotating polarizer (variable attenuator); F1 = 488 nm narrow band interference filter; L1 = diverging lens, focal length = –10 cm; DM = dichroic mirror, λ = 500 nm; L2 = scan lens (Zeiss 10× widefield eyepiece); F2 = barrier filter (515 nm long-pass color glass: Schott OG515); A = confocal aperture; L3 = converging lens, f = 5 cm; APD = avalanche photodiode module. Distance from the scan mirror in the confocal scan head to front surface of L2 is 2.0 cm; from L2 to A = 80 cm; from L2 to L1 = 70 cm, from L3 to diode detector = 5 cm. L4 = plano-concave lens, f = –10 cm; L5 = biconvex lens, f = 5 cm; M4 = partially reflecting mirror formed by coverslip in mirror mount; ND = neutral density filter wheels. All lenses in the UV path are fused silica. (**B**) A side view diagram of the scan mirror unit from the front of the microscope, drawn perpendicular to the incoming laser beam from DM. The x-scan galvanometer is mounted through a metal block (serving also as a heat sink) to a stage allowing rotation around the axis marked by the cross. A lever attached to the stage is driven by a motorized micrometer to rotate the scan mirror in the y-axis (vertical), while the galvanometer allows simultaneous fast scanning in the x-axis (horizontal). Alignment of repeated scans is achieved by a microswitch, contacted at a preset position, that gates data acquisition.

CLSM

Overview

Figure 1A shows the optical path of the CLSM to the left of the Olympus microscope. A major feature is the use of an avalanche photodiode photon counting module, which provides a greater photon detection probability (> 40% at wavelengths between 500 and 700 nm [9]) than achieved by even prismatic-face photomultiplier tubes, while possessing similar dark count rates. Furthermore, all circuitry is contained within a single small module, obviating the need for a separate high-voltage power supply and pulse discriminator.

For simplicity, the instrument is described as set up for use with fluorophores with spectra similar to fluorescein. Other excitation lines (457 and 512 nm) and emission wavelengths are readily available by appropriate selection of dichroic mirror and laser line and barrier filters. Further, the system can be easily adapted for simultaneous imaging at dual emission wavelengths by adding a second detector channel.

Fluorescence excitation path

Fluorescence excitation is derived from a 100 mW multiline argon ion laser (Omnichrome, Chino, CA, USA), bolted to the optical breadboard using custom plastic brackets (to avoid earthing hum loops interfering with electrophysiological recordings) that raise the beam height to the axis of the video port on the microscope. The output from the laser is much greater than required by the CLSM, and most recordings are made with the beam strongly attenuated. Furthermore, the laser is usually run at a low 'standby' power setting, which greatly prolongs the life of the laser tube. After passing through an electronically-controlled shutter (S1), allowing blanking of the beam between recording periods, the laser beam is directed by a beam-steering mirror (M1) through a narrow-band interference filter (F1) selecting the 488 nm emission line. A rotating polarizer (P) allows convenient attenuation of the laser power over a roughly 100-fold range, and additional neutral density filters can be placed in the light path at this point if needed. The laser beam is then expanded by lens L1 ($f = -10$ cm), so that the beam diverges to more than overfill the back aperture of the microscope objective, and is reflected by a dichroic mirror (DM; $\lambda =$ 500 nm, Omega Optical, Brattleboro, VT, USA, mounted in a Nikon filter cube) onto a galvanometer-driven scan mirror in the confocal scan head. This mirror is mounted at a conjugate telecentric plane, formed by the scan lens (L2), which comprises a widefield 10× eyepiece (Zeiss) in a custom mount fitted to the bayonet adapter on the microscope video port. The beam diameter at the scan mirror is about 2 mm, allowing use of a small mirror (3 mm square), which has low inertia and thus permits fast scan rates. Rotations of the scan mirror result in deflections in position of the diffraction-limited laser spot focussed in the specimen by the microscope objective. The maximum deflection in our system is limited by the aperture of L2, and corresponds to about two-thirds of the field viewed through the microscope oculars, or about 250 μm with a 40× objective. Brackets glued onto the base of the Olympus IX70 are used to clamp the microscope firmly in position to avoid movement and vibration from the supplied rubber feet. To assist in alignment, the microscope is mounted with the video port in line with a row of tapped holes in the breadboard, and all light paths are directed following the 1 inch grids of pre-drilled holes.

Fluorescence emission path

Fluorescence excited in the specimen by the laser beam is collected by the objective and passes back through the video port. The Olympus IX70 can be supplied with beam splitters directing light to the video port and oculars with respective ratios of either 80/20 or 100/0. We chose the former ratio because, although 20% of the fluorescence signal is lost, the ability to directly view the laser scan line in the specimen through the oculars is advantageous during experiments. The loss of 20% of the excitation light is inconsequential, as the laser power can be increased to compensate. For safety, a 510 nm long-pass color glass filter is permanently installed before the binocular microscope head, to completely block 488 nm laser light while transmitting fluorescence light. Fluorescence light passing through L2 is descanned by the galvanometer mirror, so that a stationary beam passes through the dichroic mirror and is deflected by mirrors M2 and M3 onto the detector system. The purpose of M2 and M3 is to provide a longer optical arm, so that the image of the laser spot is highly magnified at the position of the confocal aperture. Filter F2 is a 510 nm long-pass sharp cutoff color glass filter, which blocks the 488 nm laser light while transmitting fluorescence at $\lambda > 510$ nm. Use of a long-pass filter maximizes detection efficiency, but for some purposes a broad band-pass filter provides better rejection of stray light and autofluorescence at wavelengths away from the emission maximum of the fluorophore. A highly magnified (about 1000×) image of the fluorescent spot in the specimen is formed at the plane occupied by the confocal aperture A, and the z-axis resolution of the system can be optimized by varying the size of this pinhole. Because of the high magnification, the required apertures are relatively large (0.5–2 mm), and a range of sizes were made using a broken glass microelectrode to punch holes in pieces of aluminium foil. Finally, the near-parallel beam of light passing through the aperture is focussed by lens L3 ($f = 5$

cm) to a small spot centered within the active area (about 200 μm across) of the avalanche photodiode detector which, to assist in alignment, is mounted on a low-profile x–y–z micropositioner (New Focus Inc.)

To maximize light throughput, all mirror and lens surfaces are broadband dielectric coated. The small active area of the detector already provides strong rejection of stray light, and with the addition of covers over the optical path (especially between the aperture and detector), it is possible to operate the microscope under normal room lights.

Scan head

Fast x-scanning of the confocal spot is achieved by a galvanometer-based mirror positioning system (model 6800/CB6588; Cambridge Technology, Inc., Watertown, MA, USA), which is mounted in the scan head assembly (Fig. 1B) to scan the laser beam in the horizontal (x) plane. For correct operation, it is critical that the axis of the mirror is positioned at the conjugate telecentric plane imaged by the scan lens L2. This can be determined by placing a piece of frosted glass over an open position on the microscope nosepiece. When correctly adjusted, the glass should be uniformly illuminated and the laser light should not appear to move as the galvanometer mirror is scanned. Also, care should be taken to orient the galvanometer so light is reflected by the front surface of the mirror. An further important practical point is to mount the galvanometer in a holder sufficiently massive to act as an efficient heat sink, as the drive coils generate appreciable heat at high scan rates.

The moving magnet scanner is supplied together with a servo amplifier card, so that the ramp drive signal derived from the control box described above produces a linear change in scan angle, and hence linear displacement of the confocal spot. Figure 2B illustrates ramp waveforms (at a scan rate of 2 ms per line), and corresponding mirror positions reported by the optical position sensor on the galvanometer.

During experiments, it is very convenient to monitor the analogue signal from the detector on an oscilloscope, either synchronizing the oscilloscope sweep to the line

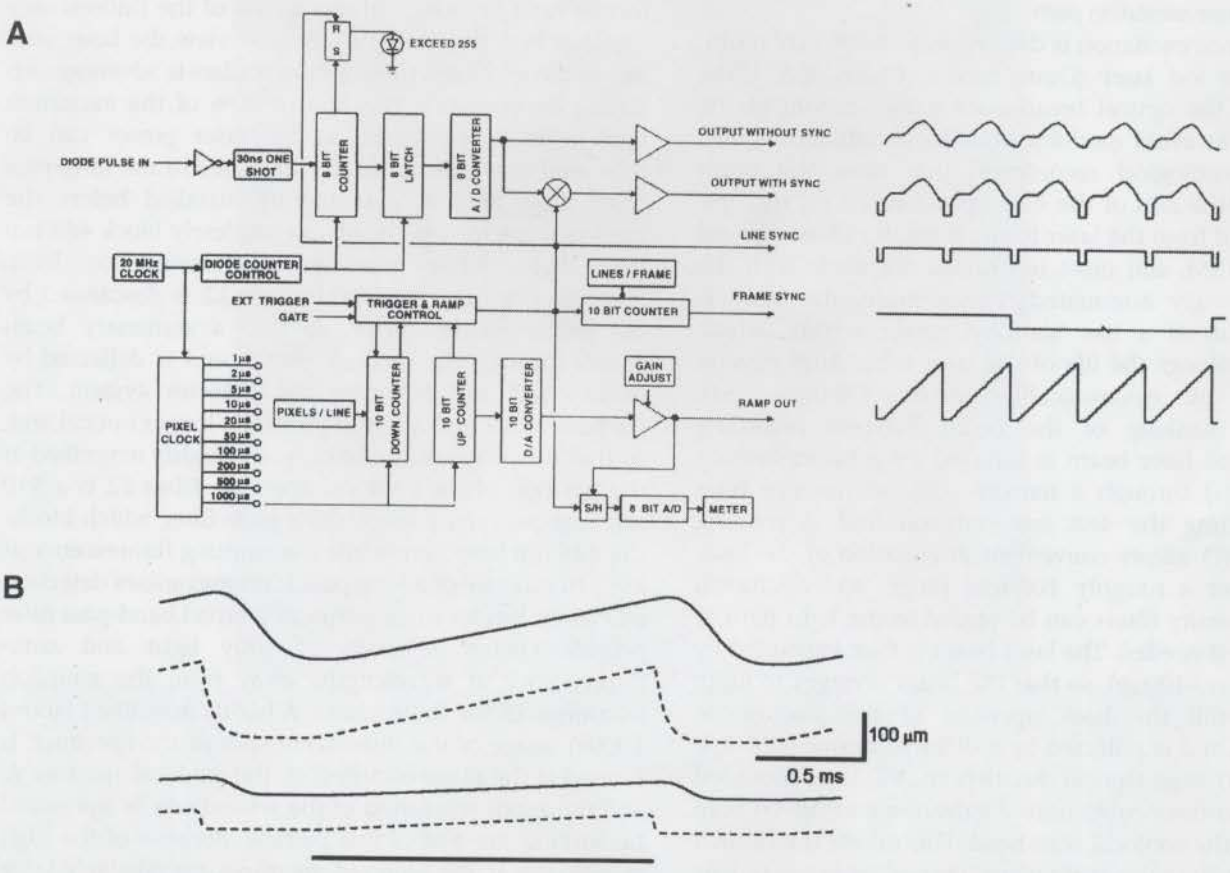

Fig. 2 (**A**) Block diagram of the mirror controller/photon counting unit and waveforms illustrating ramp drive signal and output signals. See text for further details. (**B**) Fidelity of mirror scan. Traces show ramp drive waveforms (dashed curves) and actual mirror position (solid curves) for small (lower) and large (upper) scan displacements, both at a scan rate of 2 ms per line. With a 40× objective, the galvanometer deflections correspond to 50 and 200 μm scan lengths, respectively. The horizontal bar indicates the ramp time during which image data are acquired. The flyback interval was set to 400 μs.

sync pulse or driving the y-amplifier with the ramp command signal. This provides immediate visual feedback that can, for example, be used to locate sites of Ca^{2+} release as the specimen is moved using the mechanical stage of the microscope.

Most applications we describe involve only one-dimensional (line) scanning. To permit two-dimensional scans and increase the utility of the system, however, the galvanometer is mounted on a rotation stage (Prism mount; New Focus Inc.) allowing simultaneous rotation around a horizontal axis orthogonal to, and passing through the center of the scan mirror (Fig. 1B). An arm attached to the stage is driven by a micrometer and stepper motor, allowing vertical deflection of the laser beam in the y-axis at a precise rate determined by the pulse rate of the stepper motor controller. To obtain square pixels at various 'zoom' settings, the motor speed settings are calibrated for a range of commonly used line lengths and scan rates. Movement of the micrometer drive also actuates a microswitch that gates the pixel clock input to the digitizer board, so that repeated images can be scanned beginning at the same location (within 1 'y' pixel).

This system of using a single mirror scanned around two orthogonal axes offers several advantages over dual-mirror systems. The design is simplified, light losses are minimized, and problems of alignment are greatly reduced. The only major drawback lies in the maximum speed of y-axis scanning, and particularly in the time required for 'flyback' before beginning a new scan. This, however, is not an issue for line scanning and, except at very fast pixel clock rates (< 10 μs), the speed of the stepper motor drive is not a limiting factor in the time required to acquire a single image.

Detector and electronics

The photon counting detector module (SPCM-AQ-121; EG & G Optoelectronics, Canada Ltd.) contains an avalanche photodiode, together with necessary cooling circuitry, high voltage power supply, and pulse discriminator, and only requires connection to a 5 V power supply. Models are available with various dark count rates, but for use in fluorescence recording, where there is a high basal fluorescence signal (typically > 50 000 cps in our experiments), a module with less stringent specifications (~500 dark cps) is entirely adequate. Output from the module is TTL pulses (5 ns duration), with the output rate linearly proportional (< 10% deviation) to light intensity for count rates up to 2 MHz and saturating above 15 MHz.

A custom electronics unit was designed to both process output from the detector and provide a ramp drive signal for the galvanometer driving the scan mirror (Fig. 2). This is driven by a pixel clock, which generates pulses at switch-selected intervals between 1 μs and 1 ms. During each pixel interval, photon counts from the detector are summed by an 8-bit counter. Following the next clock pulse this sum, representing the pixel intensity, is made available on both digital or analogue interfaces for sampling by a computer, and the counter is reset to zero to begin counting again. An LED provides visual warning if the pixel counts exceed the maximum count of 255. The pixel clock also drives the ramp generator used to drive the scan mirror. Pixel pulses are summed by a 16-bit counter, the output of which is continuously fed through an analog-to-digital converter to produce a linear stepwise ramp. A thumbwheel switch is used to set the desired number of pixels per scan line (1–999), and when this maximum number is reached the counter is reset to zero, a TTL pulse is sent to a 'line sync' output socket, and the mirror is returned to the starting position following a flyback waveform, which is low-pass filtered by an RC circuit to minimize overshoot and thus decrease the settling time. The length of the scan line in the specimen is adjusted by varying the gain of an amplifier placed after the analog to digital (AD) converter and, because the line length also depends on the selected number of pixels per line, a sample-and-hold circuit and digital meter are used to display the peak voltage at the maximum excursion of each line. These readings can then be readily calibrated in terms of length of scan line in microns for use with each objective lens. Finally, another counter sums line sync pulses, allowing a desired number of lines per frame to be set on a thumbwheel switch for possible future use with an automated x–y scanning system. Output waveforms from the ramp generator, sync outputs, and photon counter are illustrated in Figure 2A.

Computer software

The composite photon count output and line sync signal is digitized by a computer and stored on hard disk in throughput mode, so that gap-free records are obtained for durations limited only by the available disc space. We use the Fetchex routine in the pClamp software package (Axon Instruments) for this purpose, although other packages would also be suitable. Acquisition of signals by the AD-converter board is driven by the pixel clock output of the ramp generator/photon counting unit, so that the acquisition rate automatically matches the setting of the pixel clock switch on the ramp generator box and 'pixel jitter' resulting from free-running clocks in the ramp generator and AD-converter board is avoided. Custom routines written using the IDL programming language (Research Systems Inc.) are then used to construct and analyze images formed from the raw data files. In brief, a routine identifies the positions of line sync pulses (negative data) in the data file and forms an

image array in which successive columns represent successive line scans aligned by the rising edges of preceding sync pulses. Finally, a correction is applied for 'missed pulses' arising from the dead time of the photon counting detector module, using a look-up table based on correction factors supplied by the manufacturer.

Flash photolysis system

The system described here allows for flash photolysis of caged compounds using both point-source and wide field irradiation and can be employed either independently or in conjunction with the confocal scanner. A frequency-tripled Q-switched Nd:YAG laser (Mini-Lite; Continuum, Santa Clara, CA, USA) is used to provide brief (5 ns) pulses of UV (355 nm) light, which can be focussed down to a small (1–2 μm) spot size by the microscope objective. Sustained (tens of ms to s) irradiation over a wide field is provided by a separate xenon arc lamp source. Light from both systems is combined by a beam-splitter, and directed into the epifluorescence port of the Olympus IX70, which is equipped with a standard UV filter cube and fluor objective lenses. Note that, with the exception of the filter cube and holder, no Olympus epifluorescence components are required. The total cost of the UV photolysis system is about US$16 000, of which the greater part is accounted for by the Mini-Lite laser (US$13 500).

The upper section of Figure 1A shows the layout of the photolysis light paths. All lenses are fused silica for optimal UV transmission, and optical components are mounted to the breadboard using standard post mounts at a height corresponding to the center line of the Olympus epifluorescence port. The small size of the Mini-Lite laser head allows it to be readily mounted on the optical breadboard using an aluminium bracket. Nylon screws and insulating stand-offs are used to avoid hum-loops for electrophysiological recording. Lenses L4 and L5 form a beam expander, so that the laser beam fills the back aperture of the objective lens, thus making use of its full numerical aperture. The beam from the laser at full power setting is sufficiently powerful to damage coatings on neutral density filters and may crack an objective lens with poor UV transmission. For this reason, a microscope cover glass is used as a mirror (M4) to reflect a only small percentage of the laser beam into the microscope through a set of neutral density filter wheels (New Focus Inc.), allowing a further attenuation of up to 3.0 OD in steps of 0.1 OD. For safety, a beam dump is placed after M4 to avoid the possibility of the beam passing into the room, when covers around the laser path are removed. Alignment is facilitated by using a piece of paper marked with a yellow highlighter pen to visualize the laser beam. The laser should be turned to the low power setting, and laser safety goggles must be worn during this procedure. When correctly aligned, a marker paper placed over an open position on the microscope nosepiece should be evenly illuminated (except for interference fringes caused by reflections from both sides of the cover glass). The laser spot formed by an objective lens can then be viewed using a fluorescent-coated cover slip, and its position centered with respect to an eyepiece graticule by small adjustments of laser position and deflection of M4. Finally, the spot can be brought to a sharp focus by axial adjustment of L5, although the beam quality of the laser does not allow focussing to a diffraction-limited spot. A UV-blocking filter in the Olympus filter cube, together with the long-pass filter ($\lambda > 510$ nm) in the binocular head permit safe viewing through the microscope while the laser is in use. Nevertheless, a cover must be in place around the entire beam path (excepting a small cut-out to access the neutral density filters) to avoid the possibility of stray reflections. The laser can be operated in single-shot mode (triggered by a push switch or TTL input) or pulsed repeatedly at up to 10 Hz.

For experiments where a slow photorelease of caged compound is required over a wide area, UV light is derived from a separate arc lamp system (75 W xenon lamp, mounted in a Zeiss housing). An electronic shutter (Uniblitz; Vincent Associates, NY) controls exposure duration, and the neutral density wheels allow control of light intensity.

Laser safety

The beams of both the argon ion and Mini-Lite lasers present significant eye safety hazards, and the manufacturers' handbooks should be consulted for appropriate safety precautions. In particular, the Mini-Lite carries the highest and most dangerous Class IV classification, and is especially hazardous because the 355 nm output is invisible. General precautions are to mount the system so that laser beams are below eye level, and to place covers over all exposed beams. When covers are removed for alignment, the argon ion laser should be attenuated to the minimum intensity required to visualize the beam, and use of laser safety glasses (e.g. cat.# M38236; Edmund Scientific) is mandatory when the Mini-Lite beam is exposed. Because our systems are used by only a few, highly trained personnel, we did not implement the use of safety microswitches to shut down the lasers when covers are opened; but this precaution would be appropriate if a microscope were constructed for shared use.

Imaging of membrane structure and Ca^{2+} signals in biological preparations

Isolated rat ventricular myocytes were prepared by enzymatic dissection as described [10], and were loaded

with the fluorescent Ca^{2+} indicator Fluo–3 by incubation in a solution including 5 μM Fluo–3/AM for > 30 min. Oocytes were isolated following surgical removal of pieces of ovary from *Xenopus laevis* and, following enzyme treatment to remove surrounding cell layers, were injected using pneumatic pressure pulses with approximately 10–20 nl of a solution containing 2 mM Oregon green-1 (Molecular Probes Inc.) together with 0.2 mM caged $InsP_3$ (Calbiochem) [11]. Primary rat cortical neuronal cultures were derived from embryonic (E17-18) neocortex, with dissociated cells plated at a density of $1–2 \times 10^5$ cells/cm on polylysine-treated glass cover slips. Images of membrane structures stained with the lipophyllic fluorescent dye Di-8-ANNEPS (Molecular Probes Inc.) were obtained after placing myocytes or cultured neurons in a solution including 250–500 nM Di-8-ANNEPS (diluted 1:1000 from a stock solution in ethanol) for several minutes and then washing.

RESULTS AND DISCUSSION

Performance of the CLSM system

Resolution tests

Various approaches may be used to characterize the lateral and axial (z-axis) resolution of a confocal microscope. Primarily, it is the axial resolution that is important, because it is only in this dimension that confocal systems display large improvements over conventional wide-field microscopes. A simple test of z-axis resolution is to measure reflected light from a stationary laser spot (i.e. with the scan mirror stopped) while the microscope is focussed through a front-surface mirror [6]. Although measurements with this technique do not directly correspond to performance while imaging fluorescent biological specimens, the full-width at half-maximum intensity (FWHM) provides a number that can readily be used for comparison with other systems, and indicates whether the confocal system is correctly aligned. The data in Figure 3A show normalized reflected intensity scans as the microscope was focussed through a mirrored slide, obtained using various sizes of confocal aperture. As expected, the FWHM decreases with decreasing size of the aperture, and reduces to about 500 nm with an aperture of 0.75 mm diameter.

A more relevant and biologically useful test is to image fluorescent latex beads (green fluorescent latex microspheres: Molecular Probes Inc.) of various known sizes in aqueous medium. Intensity profiles through the center of the sub-resolution 0.1 μm beads provide measures of the point spread function of the CLSM. The FWHM of the axial and lateral point spread functions are about 300 and 400 nm, respectively; with no correction applied for the finite size of the beads (Fig. 3B). Figure 4 shows images of 2 μm (Fig. 4A,B) and 0.1 μm (Fig. 4C,D) beads obtained by axial (x-z) (upper; Fig. 4A,C) and lateral (x–y) (lower; Fig. 4B,D) scanning.

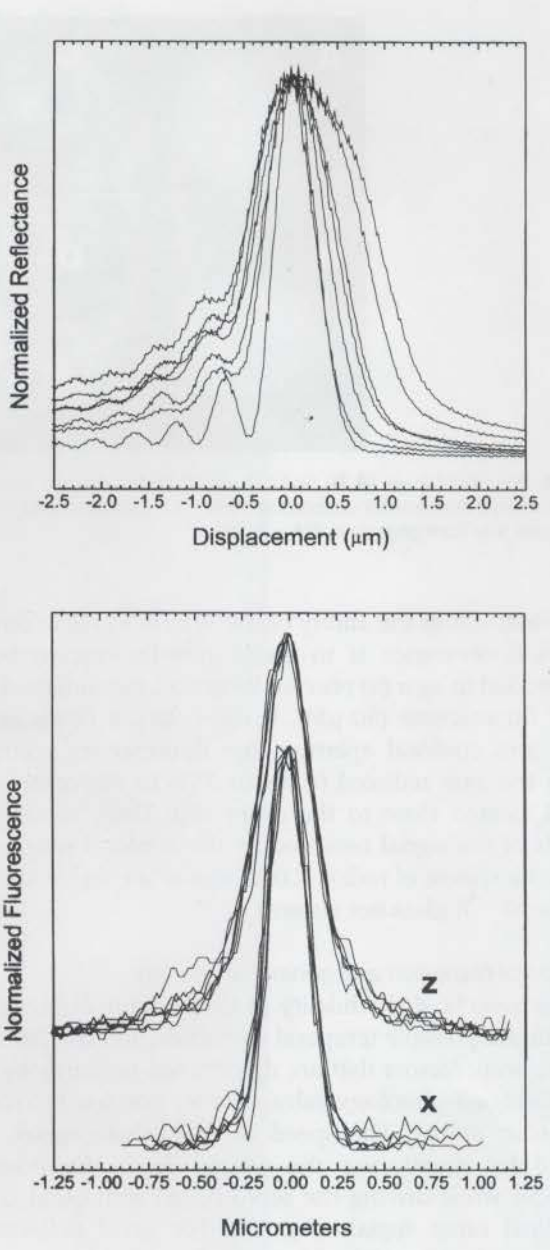

Fig. 3 Measurements of axial and lateral resolution. (**A**) Axial resolution measured in reflectance mode by focussing through a mirrored slide. Traces show normalized reflectance profiles obtained using confocal apertures with diameters of 0.5, 0.8, 1.0, 1.6, 2, 2.5, and 3 mm; the width of the profiles decreases progressively with decreasing aperture. Negative displacements correspond to focus positions beyond (above) the mirror. Nikon 60× Plan Apo objective, NA = 1.4. (**B**) Intensity profiles through 100 nm fluorescent latex beads scanning laterally (x) and axially (z) through the center of the beads. In each case, superimposed plots show profiles from six beads measured from images like those in Figure 4F. Olympus 40× fluor objective, NA = 1.35.

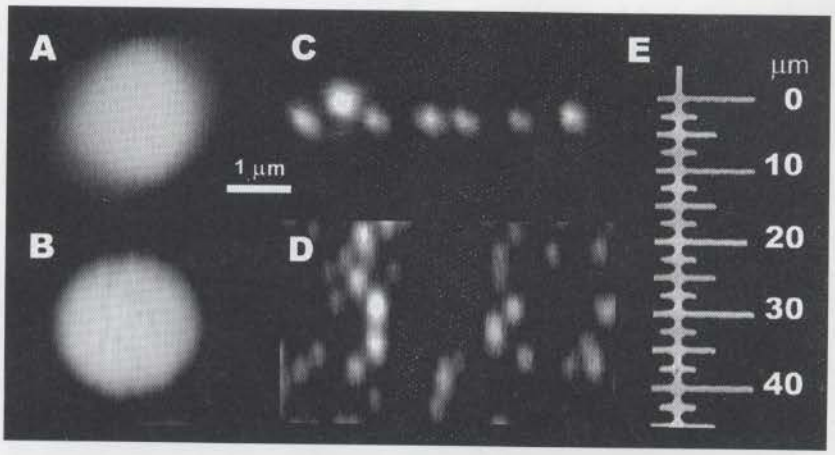

Fig. 4 Images of 2 μm (**A,B**) and 0.1 μm (**C,D**) fluorescent beads obtained by x–z (upper, A,C) and x–y (lower, B,D) scanning. (**E**) x–y scan of a mirrored micrometer calibration slide. The galvanometer mirror scan runs along the length of the graticule. All images obtained with Olympus 40× fluor objective, NA = 1.35.

A final test of the ability of the system to reject out-of-focus fluorescence is to image non-fluorescent beads embedded in agar (to prevent Brownian motion) made up with fluoresceine (50 μM). Using 0.92 μm beads and a 0.75 mm confocal aperture, the fluorescence recorded from the agar reduced to about 35% in the center of a bead located close to the cover slip. Thus, about two-thirds of the signal recorded by the confocal spot arises within a sphere of radius < 0.46 μm, or a volume of 0.5 fl (0.5×10^{-15} l) (data not shown).

Temporal resolution and geometric linearity

Other aspects of the fidelity of the imaging concern the maximum possible temporal resolution and the linearity of the scan; factors that are determined primarily by the Cambridge Technology galvanometer unit used to rotate the scan mirror. The speed of the galvanometer was tested by monitoring the output from the position encoder while driving the servo board with rapid (2 ms per line) ramp signals (Fig. 2B). For small deflections, corresponding to a 50 μm scan with a 40× objective, the flyback and settling time after each line is only about 200 μs (lower traces), but increases to about 400 μs with large (200 μm) deflections. As a compromise, we normally operate the scanner with a dead time of 400 μs following flyback, so that image data are collected for 1.6 ms of each 2 ms waveform, during the linear part of the ramp (bar in Fig. 2B). If the length of the scan line is restricted, however, it is possible to increase the scan speed to 1 ms per line and decrease the dead time to 200 μs to collect data for 800 μs each scan.

Finally, the linearity of the overall scanning system (including both the galvanometer and optics) was tested by imaging (in reflectance mode) a mirrored micrometer calibration slide (Fig. 4E). Any deviations from linearity in the image of this graticule were < 500 nm over a 50 μm scan line (i.e. < 1%). A similar performance was achieved also for scans in the y-axis.

Imaging of local Ca^{2+} transients

The confocal scanner was designed primarily for line-scan confocal recording of localized transient intracellular Ca^{2+} signals; $InsP_3$-mediated puffs in *Xenopus* oocytes [3] and sparks in cardiac cells [4,10]. These events have rapid (tens or a few hundred ms) time courses, and give Ca^{2+} signals localized to within a few microns. Thus, imaging systems with high spatial and temporal resolution are required, and use of confocal microscopy provides a particular advantage because the wide depth of field of conventional wide-field fluorescence microscopy blurs the sharply localized Ca^{2+} gradients during these events and underestimates peak changes. As described, our CLSM provides a temporal resolution as fast as 1 ms per line with a sub-micrometer spatial resolution.

Figure 5A illustrates Ca^{2+} puffs evoked in an oocyte by photoreleasing $InsP_3$ throughout a roughly 100 μm spot around the scan line by a flash of UV light provided by the arc lamp system in Figure 1B. Two puffs are visible in this example, arising independently at sites about 10 μm apart. For this application, a scan rate of 8 ms per line provided good resolution of the time course of puffs (Fig. 5B); 4 times faster than the frame rate of a conventional video system. Moreover, the record in Figure 5A,B (see the arrows) shows a Ca^{2+} 'blip' – a Ca^{2+} release event with a peak amplitude about one-fifth that of a puff, which may reflect Ca^{2+} flux through a single $InsP_3$ receptor [11]. These events were too small to resolve previously in video-rate confocal images obtained using a Noran Odyssey system [3], although they could be detected by

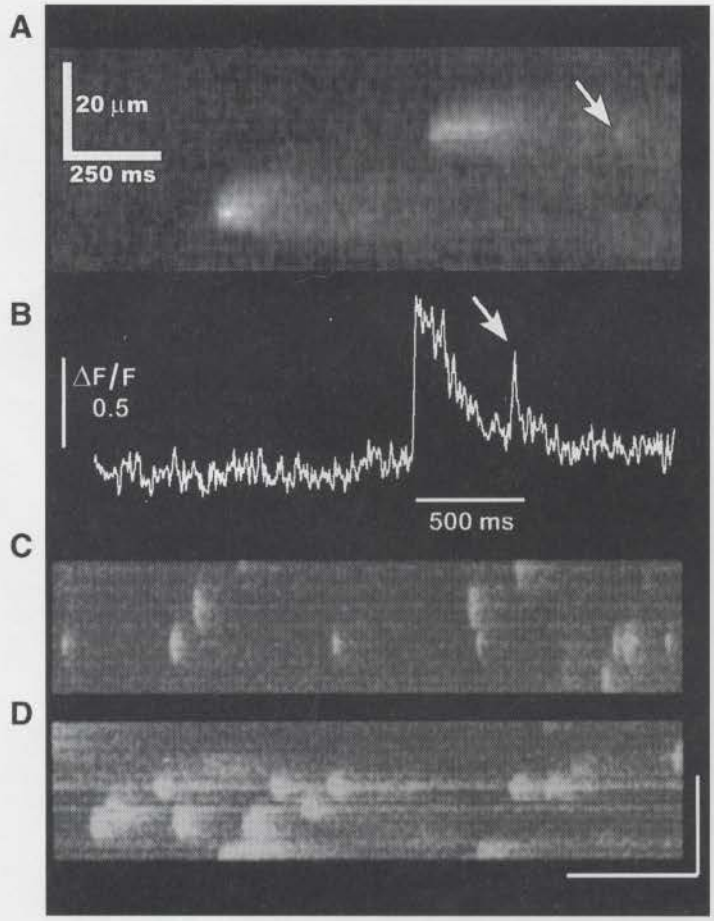

Fig. 5 Localized Ca^{2+} transients recorded in line-scan mode in *Xenopus* oocytes (**A,B**) and isolated rat ventricular myocytes (C,D). In all line-scan images, the distance along the scan line is depicted vertically, and successive scan lines at intervals of 4 ms (A,B) or 3 ms (C,D) are stacked from left to right. (**A**) Image shows two Ca^{2+} puffs arising at sites about 10 μm apart in an oocyte. The oocyte was loaded with Oregon green-1 and caged $InsP_3$ to respective intracellular concentrations of about 50 μM and 5 μM, and Ca^{2+} release was evoked by a photolysis flash uniformly illuminating a 100 μm diameter spot centered around the scan line at the start of the record. The image shows fractional increases in fluorescence (ΔF/F) after ratioing by the averaged resting fluorescence along the scan line and after smoothing by a 3 × 3 pixel median filter. The arrow marks a small transient Ca^{2+} signal ('blip') occurring at the upper site shortly after a much larger puff. (**B**) Intensity profile (ΔF/F) measured as a function of time at the upper puff site. Data are averaged over 5 pixels along a line at the point of the arrow in (A). The blip noted in (A) is marked by an arrow. (**C, D**) 'Raw' fluorescence images, without ratioing, showing spontaneous Ca^{2+} sparks in ventricular myocytes scanned along the axis of a cell (**C**) and transversely across a different cell (**D**). Calibration bars indicate 10 μm and 500 ms. The broader appearance of some sparks in (D) results from synchronous activation arising at multiple transverse sites. Images in (C,D) are reproduced from [12] with permission of *The Journal of Physiology*.

monitoring fluorescence from a stationary laser spot [11]. Their resolution in linescan images permits detailed spatial, as well as temporal, studies of blips.

Another test is provided by measurement of Ca^{2+} sparks in cardiac myocytes, which show appreciably faster time courses than puffs. Figure 5C shows an image of spontaneous sparks obtained by scanning longitudinally along the length of a myocyte at a rate of 3 ms per line. The CLSM provided images of sparks with both better spatial resolution and signal-to-noise ratio than in previous studies under similar conditions using BioRad MRC 600 instruments (compare, for example, spark images in [10] obtained with an MRC600 to those in [12] obtained with the present system). Furthermore, in scans oriented transversely across the myocyte, the superior spatial resolution of the CLSM allowed the dissection of sparks into yet smaller elementary release events, occurring in near synchrony at sites spaced along z-lines at separations of several hundred nanometers (Fig. 5D; and see [12]). A final advantage is provided by the ability to record linescan data continuously for indefinite periods, as compared to the roughly 1 s limit imposed by the single-frame recording mode of the MRC 600. Thus, the activity of individual Ca^{2+} release sites can be monitored for prolonged periods, and has revealed that individual sites may undergo long-term changes in 'mode' or frequency of spark generation (I. Parker & W.G. Wier; unpublished data).

x–y imaging

Although the confocal scanner was built primarily for use in linescan mode, addition of a y-axis scanner to rotate the scan mirror readily allows high-resolution x–y images to be obtained. In particular, the spatial resolution is close to the diffraction-limited performance expected for a confocal microscope [13], and the user has complete control over the desired pixel resolution (up to 1000 × 2000 pixels in our present system).

Reproducibility between repeated scans is within 1–2 pixels (< 250 nm with a 40× objective). A 1000 × 1000 pixel image takes about 21 s to acquire using a pixel dwell time of 20 μs, and the maximum speed of the stepper motor driving the y-scan allows fields of up to 250 μm (with 40× objective) to be scanned at this frame rate. Images with lower resolution can be acquired with correspondingly shorter scan times, though the maximum frame rate is limited also by the time required to return to the starting y-position. With our present stepper motor this takes about 9 s for a 100 μm scan.

Examples of x–y images are shown in Figure 6. The pollen grain in Figure 6A is a readily available specimen, with which the performance of the microscope may be compared to other systems. The image of a cardiac myocyte (Fig. 6B) stained with Di-8-ANNEPS to label the surface and transverse axial tubular membrane systems provides a good demonstration of the available resolution using the confocal microscope to obtain an

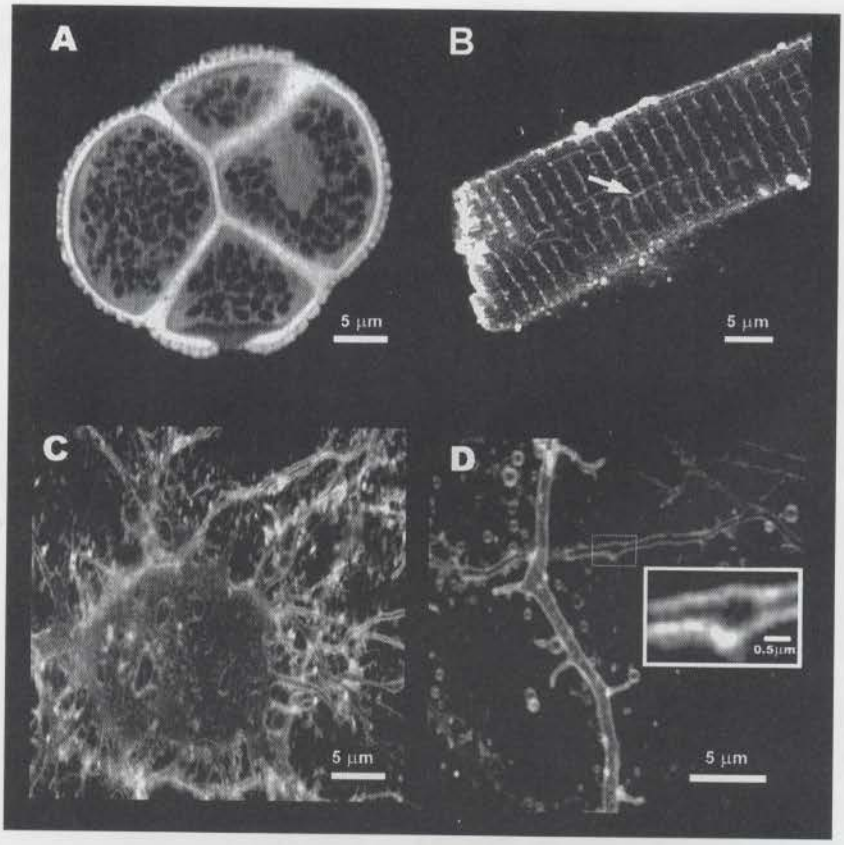

Fig. 6 Confocal images of various biological preparations, illustrating the confocal sectioning ability and lateral resolution. (**A**) Section through the center of a pollen grain (mixed pollen grains slide wm B690; Carolina Biological Supplies). (**B**) Section through the center of a live, isolated rat cardiac myocyte, stained with Di8-ANNEPS to visualize surface and transverse axial tubular membranes (see arrow). (**C, D**) Images of cultured cortical neurons stained with Di8-ANNEPS to visualize surface membranes, showing cell soma and processes at various magnifications (see inset). A, C and D were obtained with Olympus 40× fluor objective and B with a Nikon 60× PlanApo objective.

optical section through the center of a relatively thick (about 20 μm) cell. Tubular membrane structures (which are 50 nm across by electron microscopy) show an apparent width in the image of approximately 200 nm, and longitudinal tubules are clearly evident (arrowed). These latter structures were not apparent in images obtained using an MRC 600 system, and were less well resolved than in Figure 6B in images from a Zeiss CLSM. Finally, Figure 6C,D shows images of cultured cortical neurons stained with Di-8-ANNEPS at various magnifications. Note in Figure 6D that the thin optical section allows a clear visualization of processes < 1 μm diameter passing over each other. Also, in a section through a fine process < 600 nm across, it is possible to resolve separate membranes on each side, with the apparent thickness of the membranes being approximately 200 nm.

A further comparison of the resolution of our system with commonly used commercial CLSM is shown in Figure 7, which shows 'spiky' pollen grains imaged using a Noran Odyssey and BioRad MRC1024 systems as well as our instrument. Even when optimized with a small confocal aperture, the Noran gave relatively poor rejection of out-of-focus fluorescence and resolution of structures within the spikes (Fig. 7B), although it should be noted that the slit-scanning design of this instrument emphasizes scanning speed at the expense of axial resolution. Images obtained with the BioRad were appreciably better (Fig. 7C), but even with the confocal aperture set slightly smaller (1.6) than the manufacturer's recommendation, the optical sectioning ability and resolution of fine structure were still inferior to our 'homebrew' system (Fig. 7D). Furthermore, despite setting the laser power to maximum, images with the BioRad were more 'noisy' (i.e. fewer photon counts per pixel).

Imaging of signals evoked by point-photolysis of caged precursors

Use of the laser UV photolysis system together with the CLSM provides a versatile tool for localized optical stimulation of cells and imaging of resulting physiological

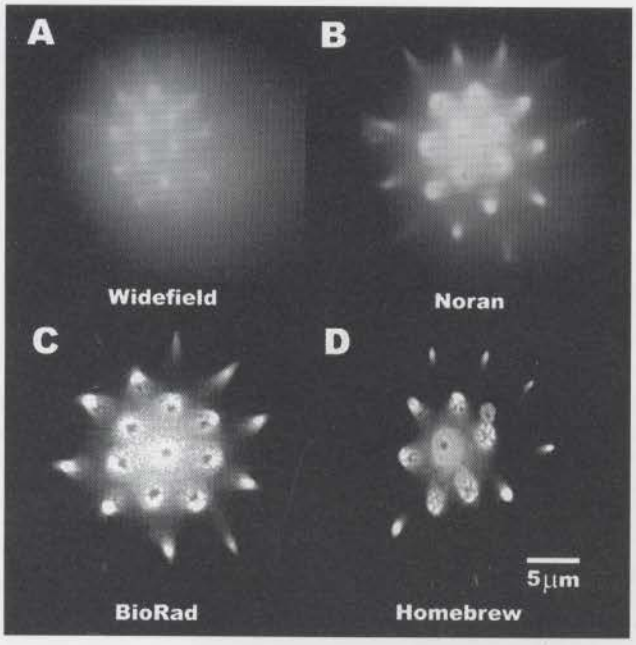

Fig. 7 Comparison of the spatial resolution of x–y images obtained using our system and two commercial CLSM. The specimens are size matched stellate pollen grains, in which hollow conical 'spikes' protrude from a spherical body, reminiscent of a medieval weapon. A good test of axial resolution is provided by the ability of the CLSM to section through the spikes while rejecting out-of-focus fluorescence from the body. (**A**) A 'widefield' image, obtained using a Noran Odyssey system with the confocal aperture removed. (**B**) Image showing the best confocal resolution that could be obtained with the Noran Odyssey (25 μm confocal slit, average of 128 video frames, Olympus IMT2 microscope with 40×, NA 1.3 oil immersion objective). (**C**) Image obtained with a BioRad MRC1024 system under optimal conditions (1.6 mm confocal aperture, slow scan, 1000 × 1000 pixel resolution, Nikon Diaphot microscope with 60× Plan Apo oil immersion objective). (**D**) Image obtained with our 'homebrew' CLSM. Note the better rejection of out-of-focus fluorescence and greater detail in the structure of spine walls.

responses. Two applications are illustrated in Figure 8. In Figure 8A, the UV spot was focussed in a droplet of caged fluoresceine (Molecular Probes Inc.), and the resulting liberation of free fluoresceine following a single flash was imaged along a scan line centered on, and confocal with, the UV spot. Fluorescence rose immediately (within the 2 ms line scan period) following the laser flash and was distributed over a radial distance of roughly 3 μm in the first line scanned after the flash. Most of this spread probably resulted from rapid diffusion, because the focal laser spot viewed using a fluorescent slide is < 2 μm in diameter. During subsequent scan lines, the fluorescence became more diffuse and fainter as fluoresceine diffused away from the irradiated region.

A second example (Fig. 8B) shows Ca^{2+} liberation evoked in a *Xenopus* oocyte by localized photorelease of $InsP_3$. The oocyte was loaded with caged $InsP_3$, together with Oregon green-1 to monitor Ca^{2+} signals, and the microscope was focused 7 μm into the cell at a depth where Ca^{2+} release sites are concentrated [3]. With a laser intensity about 4 times that required to evoke any detectable response, Ca^{2+} liberation began following a latent period of roughly 30 ms after the flash and was initially restricted to a region about 10 μm across, but then expanded to encompass a > 50 μm region. The generation of this signal reflected a combination of several processes, unlike the simple diffusion of fluoresceine in Figure 8A. First, $InsP_3$ diffused from a near point-source and was subsequently degraded by cellular enzymes. Secondly, Ca^{2+} liberation was evoked following a latent period that varies with [$InsP_3$] and, in turn, Ca^{2+} ions in the cytosol were subject to diffusion, buffering, and reuptake. Thus, experiments like that in Figure 8B provide a means to locally elevate [$InsP_3$] in small subcellular regions and explore regional variations in sensitivity to this second messenger, as well as the factors determining its 'range of action' [14].

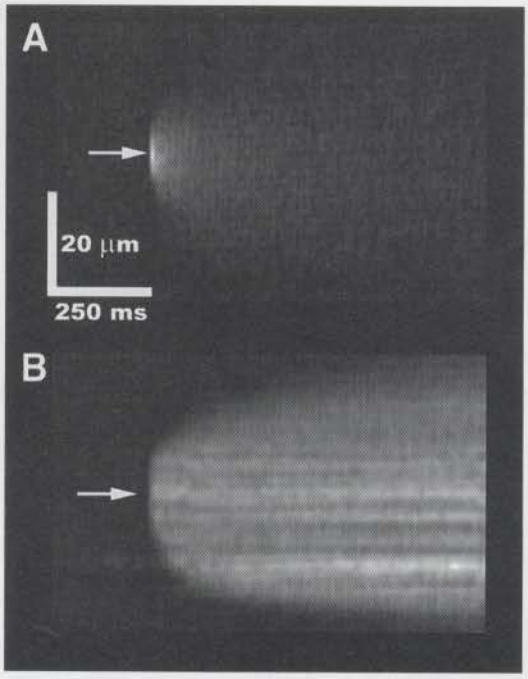

Fig. 8 Examples of use of the CLSM in line-scan mode to image signals evoked by point photolysis of caged precursors by the UV laser system. In both cases, the UV laser spot was aligned with the center of the scan line, and the arrows mark the position and time of the photolysis flash. Images show fractional increases in fluorescence (ΔF/F) after ratioing by the resting fluorescence before stimulation. (**A**) In vitro photolysis of caged fluoresceine. A droplet of caged fluoresceine (50 μM) was placed on a coverslip, and the microscope was focussed about 2 μm into the droplet. (**B**) Ca^{2+} release evoked in a *Xenopus* oocyte by photorelease of $InsP_3$. The oocyte was loaded with Oregon green-1 and caged $InsP_3$ to respective intracellular concentrations of approximately 50 μM and 5 μM, and recordings were made with the microscope focussed at a depth of about 7 μm into the cell.

One practical problem with the use of a frequency-tripled NdYAG laser for photolysis is that, because of the very short (5 ns) flash duration, the pulse energy is high and may lead to significant local heating and damage to the cell when the beam is focussed down to a small spot. In experiments with oocytes, we found that damage occurred if the attenuator was set to OD values less than about 0.5–1 (40× NA 1.35 objective; Mini-Lite laser on full power setting), and was evident as a local elevation of $[Ca^{2+}]$ that persisted for many seconds or minutes after a flash. By injecting oocytes to achieve appropriate intracellular concentrations of $InsP_3$ (about 20 μM), however, it was possible to photorelease sufficient $InsP_3$ to generate large Ca^{2+} responses while using flash intensities only a few percent of the damage threshold.

CONCLUSIONS

The main purpose of this paper is to show that it is possible to construct a confocal microscope that offers a performance at least as good, or better, than comparable commercial instruments. Moreover, the cost of the system is much lower than commercial instruments, and no more than that of a good 'wide-field' video fluorescence system. No new principles are involved in our instrument, and its performance is bounded by the same diffraction limits that apply to any other confocal microscope. Nevertheless, much depends in practice upon the details of implementation, and our experience is that design constraints and improper alignment of many commercial instruments frequently lead to their providing a resolution appreciably lower than the theoretical limit. In particular, inefficiencies in light detection often force the use of wide confocal apertures (thus impairing axial resolution) and provide a poor signal-to-noise ratio for temporal resolution of dynamic signals. Furthermore, use of complex light paths hinders accurate alignment by the user. These problems are mitigated in our instrument by employing an avalanche diode with a detection efficiency higher than any other available detector system, and by designing a relatively simple light path. In addition to the enjoyment and satisfaction gained by building one's own instrument, construction of the microscope instills an excellent working knowledge of how to keep the system aligned and functioning optimally. We originally constructed the microscope for line-scan imaging of sub-cellular Ca^{2+} transients, though the excellent spatial resolution makes it attractive also for morphological studies. Indications of its performance for the former purpose are provided by the resolution of Ca^{2+} sparks in cardiac cells into discrete release events at sites at sub-micrometer spacings [12], and by the imaging of elementary Ca^{2+} blips in oocytes (Fig. 5A), which may represent single channel activity [11].

In addition, we describe a laser/arc lamp UV system for flash photolysis of caged compounds. This can be used as a stand-alone unit but, in conjunction with the CLSM, forms a versatile and powerful tool for opto-physiological study of many cellular processes.

ACKNOWLEDGEMENTS

We thank Jeff Michaels for help in designing and constructing the electronics, Drs Wei-Jin Zang and Xiao-Ping Sun for assistance with experiments, and Jennifer Kahle for editorial help. Financial support was provided by NIH grants to IP (GM48071) and WGW (HLBI29473 and HLBI55280).

REFERENCES

1. Pawley J.B. Handbook of Biological Confocal Microscopy. New York: Plenum, 1995.
2. Parker I., Yao Y. Regenerative release of calcium from functionally discrete subcellular stores by inositol trisphosphate. Proc R Soc Lond [Biol] 1991; **246**: 269–274.
3. Yao Y., Choi J., Parker I. Quantal puffs of intracellular Ca^{2+} evoked by inositol trisphosphate in Xenopus oocytes. J Physiol (Lond) 1995; **482**: 533–553.
4. Cheng H., Lederer W.J., Cannell M.B. Calcium sparks: elementary events underlying excitation-contraction coupling in heart muscle. Science 1993; **268**: 1045–1049.
5. Bootman M.D., Berridge M.J. The elemental principles of calcium signals. Cell 1995; **83**: 675–678.
6. Pawley J.B. Fundamental limits in confocal microscopy. In: Pawley J.B. (Ed) Handbook of Biological Confocal Microscopy. New York: Plenum, 1995; 19–36.
7. Lerner E.J. Avalanche photodiodes can count the photons. Laser Focus World 1996; **32**: 93–102.
8. Art J. Photon detectors for confocal microscopy. In: Pawley J.B (Ed) Handbook of Biological Confocal Microscopy. New York: Plenum, 1995; 183–195.
9. MacGregor A. Silicon avalanche photodiodes for low-light, high-speed systems. In: Photonics Design and Applications Handbook, 1993; H 111–114.
10. Lopez-Lopez J.R., Shacklock P.S., Balke C.W., Wier W.G. Local stochastic release of Ca^{2+} in voltage-clamped rat heart cells: visualization with confocal microscopy. J Physiol (Lond) 1994; **480**: 21–29.
11. Parker I., Yao Y. Ca^{2+} transients associated with openings of inositol trisphosphate-gated channels in Xenopus oocytes. J Physiol (Lond) 1996; **491**: 663–668.
12. Parker I., Zang W-J., Wier W.G. Ca^{2+} sparks in cardiac cells involve synchronous Ca^{2+} release from multiple sites. J Physiol (Lond) 1996; **497**: 31–38.
13. Inoue S. Foundations of confocal scanned imaging in light microscopy. In: Pawley J.B. (Ed) Handbook of Biological Confocal Microscopy, New York: Plenum, 1995; 1–17.
14. Allbritton N.L., Meyer T., Stryer L. Range of messenger action of calcium ion and inositol trisphosphate. Science 1992; **258**: 1812–1815.